Metabolomic Analysis of SCD During Goose Follicular Development: Implications for Lipid Metabolism

Xin Yuan
Sichuan Agricultural University https://orcid.org/0000-0002-7130-5990
Shenqiang Hu
Sichuan Agricultural University
Liang Li
Sichuan Agricultural University
Hehe Liu
Sichuan Agricultural University
Hua He
Sichuan Agricultural University
Jiwen Wang (wjw2886166@163.com)
Sichuan Agricultural University

Research

Keywords: Stearoyl-CoA, goose follicular development, lipid metabolism, granulosa cells, SCD overexpression, SCD knockdown

Posted Date: August 5th, 2020

DOI: https://doi.org/10.21203/rs.3.rs-51158/v1

Version of Record: A version of this preprint was published at Genes on August 26th, 2020. See the published version at https://doi.org/10.3390/genes11091001.

Abstract

Background

Stearoyl-CoA desaturase (SCD) is known to be an important rate-limiting enzyme in the production of MUFA. The role of this enzyme in goose follicular development is poorly understood. To investigate the metabolic mechanism of SCD during goose follicular development, we observed SCD expression patterns during follicular development in vivo and in vitro using quantitative reverse-transcription (qRT)-PCR. Liquid chromatography-tandem mass spectrometry (LC-MS/MS) was used to determine a cellular model of *SCD* function in granulosa cells (GCs) via *SCD* overexpression and knockdown.

Results

qRT-PCR analysis showed that *SCD* was abundantly expressed in the GC layer, and was upregulated in preovulatory follicles. Peak expression was found in F1 and prehierarchal follicles with diameters of 4–6 mm and 8–10 mm, respectively. We further found the mRNA expression and corresponding enzyme activity to occur in a time-dependent oscillation in vitro, beginning on the first day of GC culture. By using LC-MS/MS, we identified numerous changes in metabolite activation and developed an overview of multiple metabolic pathways, ten of which were associated with lipid metabolism and enriched in both the overexpressed and the knockdown groups.

Conclusions

We confirmed cholesterol and pantothenol or pantothenate as potential metabolite biomarkers for studying SCD-related lipid metabolism in goose GCs.

Background

An important rate-limiting enzyme in lipogenesis is stearoyl-CoA desaturase (SCD), which synthesizes monounsaturated fatty acids (MUFAs) from saturated fatty acids (SFAs) by introducing a cis-double bond to fatty acyl-CoAs [1]. The products of SCD are major substrates for the biosynthesis of endogenous polyunsaturated fatty acids (PUFAs) and complex lipids such as triglycerides, phospholipids, cholesterol esters, and wax esters [2]. The ratio of SFAs to MUFAs can influence a broad spectrum of cellular functions; thus, the content and distribution of SFAs and MUFAs within the cell must be tightly controlled by SCD [3]. Furthermore, SCD is an integral membrane protein of the endoplasmic reticulum, where it undergoes rapid turnover in response to a variety of nutritional and hormonal signals [4] and has served a vital metabolic function during evolution [5]. Research in recent years has revealed the influence of SCD on membrane fluidity, lipid metabolism, and energy metabolism [6–8]. Therefore, SCD has been identified as an important metabolic control point and is emerging as a promising therapeutic target in the treatment of obesity, diabetes, and other metabolic diseases [3, 9]. Moreover, some studies point to SCD as a main factor in the control of cancer cell growth [10, 11].

Lipid metabolism plays an important biological role in living cells [12], including follicular cells. Investigations of lipid profiles in both follicular cells (including cumulus, granulosa, and theca cells) and follicular fluid by mass spectrometry (MS) suggest that lipid metabolism is pivotal for follicular development and oocyte maturation [13, 14]. Moreover, lipid metabolism in granulosa cells (GCs) is considered to be indispensable for oocyte maturation in bovine, sheep, and human [15–17]. In a previous study, we confirmed for the first time that de novo lipogenesis (DNL) occurs in goose GCs [18]. More importantly, we identified miRNA–mRNA interaction pairs related to the regulation of lipid metabolism in goose follicular development [19]. As the capacity of oocytes to utilize glucose as the main energy source is limited [20], lipid metabolism in GCs is considered to be indispensable for oocyte maturation. While studies have demonstrated that SCD is an important rate-limiting enzyme in lipid metabolism, research into avian follicular development and oocyte maturation, which manifest some peculiarities, is currently lacking. It has been speculated that endogenous MUFA synthesis yields a source that is distinct from the dietary MUFA pool, and acts as a metabolic switch that influences the balance of energy storage versus energy oxidation [21, 22]. Nevertheless, the mechanism by which energy status affects avian ovarian follicular selection, as well as follicular recruitment and growth, has not been thoroughly investigated and is not yet fully elucidated.

Indigenous Tianfu goose (*Anas cygnoides*) is a commercially important farm animal in southern China. However, the poor egg-laying performance is a hindrance to the industry [23]. The goose ovary contains a hierarchy of large preovulatory follicles (designated F1-F5) and a small cohort of prehierarchal follicles (Figure. 1A). The largest follicle (Fl) ovulates before the others, and F2 then replaces F1 as the dominant follicle and ovulates 48 h later. This process is successively repeated by F3–F5. Unlike mammals, however, all follicles within this cohort do not undergo atresia [24]. The prehierarchal follicles are categorized by size (2–4, 4–6, 6–8, and 8–10 mm in diameter). Follicular recruitment from the prehierarchal cohort is initiated in the 4–6 mm follicle, and follicular selection within the preovulatory hierarchy occurs

on a cohort of prehierarchal follicles (8–10 mm follicle). Understanding the mechanisms through which the processes associated with follicular recruitment and selection occur has great value for follicular development research [25].

Metabolomics is defined as the characterization and quantification of small molecules that are mediators and products of metabolism, with the aim of monitoring metabolism and its fluctuations in biological samples [26]. Therefore, metabolomic studies provide insights regarding variations in levels of endogenous metabolites as a living system responds to biological stimuli or genetic modification [27]. The overall goal of this study was to elucidate the underlying metabolites and pathways that are activated in goose GCs during follicular development using a metabolomic approach by creating a cellular model of SCD function. We analyzed the SCD expression patterns in goose follicles in vivo and in vitro by quantitative reverse-transcription PCR (qRT-PCR), and applied liquid chromatography-tandem mass spectrometry (LC-MS/MS) to investigate the effects of metabolic alterations, particularly those related to lipids, on goose follicular development.

Methods

Goose follicle collection and primary GC culture

Geese (from a maternal line of Tianfu goose) were raised under natural temperature and light conditions at the experimental waterfowl breeding farm of Sichuan Agricultural University. For follicle collection, six geese showing regular laying schedules were randomly selected as experimental samples and sacrificed 2 h after oviposition by post-anesthesia exsanguination. A pool of ovarian follicles was immediately collected from the goose abdominal cavities and placed into sterile normal saline. The follicles were then divided into groups according to their sizes (< 2, 2–4, 4–6, 6–8, and 8–10 mm in diameter) and stages of follicular hierarchy (F5, F4, F3, F2, and F1) according to previously reported nomenclature [28]. The outer connective tissue was removed from the follicles, which were then bisected to allow the yolk and adhering granulosa layer to flow out. The granulosa and theca layers were isolated as previously described [29]. They were then washed three times with PBS, quickly frozen in liquid nitrogen, and stored at − 80 °C for RNA extraction.

For primary GC culture, the granulosa layer was dispersed by incubation in 0.1% type II collagenase (Sigma, USA) in Dulbecco's Modified Eagle Medium (DMEM, HyClone, USA) for 10 min in a 37 °C water bath. After incubation, the cells were dispersed with a pipette and pelleted by centrifugation at 1000 × g for 10 min (20 °C). The supernatant was discarded, and the cells were re-suspended in 3 ml of fresh basic medium without collagenase and centrifuged. The washing procedure was repeated twice. The GCs were dispersed in DMEM supplemented with 1% antibiotic/ antimycotic solution (Solarbio, China) and 3% fetal bovine serum (Gibco, USA). The number and viability of GCs were determined with a hemocytometer using the trypan blue exclusion assay. Viability of all GCs was greater than 90%. Cells were incubated in a water-saturated atmosphere of 95% air and 5% CO_2 at 37 °C in an incubator (Thermo, USA).

RNA extraction and qRT-PCR

Total RNA was extracted using Trizol reagent (Invitrogen, USA) according to the manufacturer's instructions. The first-strand cDNA was synthesized from 1 μg of total RNA using a cDNA synthesis kit (Takara, Japan). qRT-PCR was conducted using synthesized cDNA with the SYBR PrimeScript RT-PCR kit (Takara, Japan) in the CFX96™ Real-Time System (Bio-Rad, USA); sets of gene-specific forward and reverse primers are listed in Table S1. Relative mRNA expression was determined using the $2^{(-\Delta\Delta Ct)}$ method [30]. β-actin and GAPDH mRNA levels were used to normalize mRNA levels.

Modulation of SCD with small interfering RNA

Specific small interfering RNA (siRNA), used to silence *SCD* expression, was synthesized by GenePharma (Shanghai, China) and was transfected into GCs using the Lipofectamine™ RNAiMAX Transfection Reagent (Invitrogen Co.) according to the manufacturer's recommendations. Briefly, the GCs were grown in medium (DMEM) without antibiotics one day before the experiment. On the day of transfection, pre-prepared siRNA-RNAiMAX complexes and incubated for 5 min at room temperature. The cells that we had prepared for *SCD* knockdown were removed from their medium and placed onto medium that was free of serum or antibiotics. The cells were then incubated with the siRNA-RNAiMAX complexes at 37 °C for 24, 48, and 72 h. siRNAs were delivered to cells at a final concentration of 20 nmol/L. Cells were collected for mRNA analysis to verify gene knockdown. Scrambled siRNA was used as a nonspecific negative control (NC). The following siRNA molecules were used: sense (5'-3') UUCUCCGAACGUGUCACGUTT, antisense (5'-3') ACGUGACACGUUCGGAGAATT (scrambled) as the control, sense (5'-3') GCGAUACGUCUGGAGGAAUTT, antisense (5'-3') AUUCCUCCAGACGUAUCGCTT (siRNA210), sense (5'-3') GCGGAUCUUCUUGACUAUUTT, antisense (5'-3') AAUAGUCAAGAAGAUCCGCTT (siRNA405), and sense (5'-3') GCUCAACGCCACUUGGCUATT, antisense (5'-3') UAGCCAAGUGGCGUUGAGCTT (siRNA774).

Overexpression of SCD with recombinant vector

To generate GFP-SCD, the RNA was obtained from normal goose ovarian tissue and used to generate cDNA clones of the *SCD* gene. A 981-bp cDNA fragment (GenBank Accession No. XM_013201691.1) was amplified using primers capped with XhoI and HindIII recognition sequences (Forward: 5'- CCGCTCGAGATGGAGAAGGACTTACTCAGTCATG – 3'; Reverse: 5'- CCCAAGCTTTCAGCCGCTCTTGTGACTCCC – 3'). This fragment was then inserted to construct the pEGFP-N1 plasmid. The construct was confirmed by enzymatic digestion and DNA sequencing. In the transient transfection experiment, 1 μg of the plasmid DNA was transfected into 1×10^6 GCs in six-well dishes using Lipofectamine® 3000 (Invitrogen Co) according to the manufacturer's instructions; a GFP vector and an empty control served as negative controls. The expression levels of *SCD* mRNA were detected 24, 48, and 72 h later in order to evaluate transfection efficiency.

Determination of SCD activity

The SCD activity was measured using the Goose Stearoyl-CoA Desaturase Activity Assay Kit (NJJCBIO, China). Briefly, each cell culture medium was diluted five times with sample diluent; 50 μl of the resultant dilution was then added to the enzyme label plate. Plates were incubated at 37 °C for 30 min, washed five times with wash buffer, and air-dried at room temperature. Standard reagent (50 μl) was added to the plates, which were then washed five times. After adding 50 μl reagent A and 50 μl reagent B, the plates were incubated at 37 °C for 10 min in the dark. Finally, 50 μl stop buffer was added; the optical density (OD) value was then measured by microplate reader at a wavelength of 450 nm and calculated.

Cell sample preparation for metabolomics

In total, 18 samples consisting of three biological replicates were randomly and independently analyzed to reduce analysis bias. After the samples were thawed on ice, 1 mL pre-cooled extractant (70% methanol aqueous solution) was added and whirled for 1 min. The mixture was placed in liquid nitrogen for 3 min, removed from ice for 3 min, and whirled for an additional 2 min. This procedure was repeated three times. The mixture was again centrifuged at 12000 r/min at 4 °C for 10 min, and then the supernatant was collected into the sample bottle for LC-MS/MS analysis.

High-performance liquid chromatography (HPLC) conditions

All samples were randomly analyzed to reduce analysis bias; the sample extracts were analyzed using a liquid chromatography-electrospray ionization-tandem mass spectrometry (LC-ESI-MS/MS) system (UPLC, Shim-pack UFLC SHIMADZU CBM A system, https://www.shimadzu.com/; MS, QTRAP® System, https://sciex.com/). The analytical conditions were as follows: UPLC column (Waters ACQUITY UPLC HSS T3 C18; 1.8 μm, 2.1 mm × 100 mm); column temperature, 40 °C; flow rate, 0.4 mL/min; injection volume, 2 μL; solvent system, water (0.04% acetic acid): acetonitrile (0.04% acetic acid); gradient program, 95:5 V/V at 0 min, 5:95 V/V at 11.0 min, 5:95 V/V at 12.0 min, 95:5 V/V at 12.1 min, and 95:5 V/V at 14.0 min.

Quality control (QC) samples comprised a mixture of extracts from each sample; this mixture was divided into three samples, which were analyzed using the same method as for the experimental samples. The mixed samples were injected after every five experimental samples throughout the analytical run to provide a set of data from which repeatability could be assessed.

ESI-QTRAP-MS/MS

Linear ion trap (LIT) and triple quadrupole (QQQ) scans were conducted on a triple quadrupole linear ion trap mass spectrometer (QTRAP® LC-MS/MS System) that was equipped with an ESI Turbo Ion-Spray interface, operating in positive and negative ion mode, and controlled by Analyst 1.6.3 software (Sciex). The ESI source operation parameters were as follows: source temperature 500 °C; ion spray voltage (IS) 5500 V (positive), − 4500 V (negative); ion source gas I (GSI), gas II (GSII), and curtain gas (CUR) were set at 55, 60, and 25 psi, respectively; the collision gas (CAD) was high. Instrument tuning and mass calibration were performed with 10 and 100 μmol/L polypropylene glycol solutions in QQQ and LIT modes, respectively. A specific set of multiple reaction monitoring (MRM) transitions were performed for each period according to the metabolites eluted within this period.

Qualitative and quantitative analysis of metabolites

Qualitative analysis of primary and secondary MS data was carried out by comparing the accurate precursor ion (Q1) and product ion (Q3) values, retention time (RT), and fragmentation patterns with those obtained by injecting standards under identical conditions for available standards (Sigma-Aldrich, USA http://www.sigmaaldrich.com/united-states.html), or by using a self-compiled database (MWDB; MetWare Biological Science and Technology Co., Ltd. Wuhan, China). The quantitative analysis of metabolites was based on the MRM mode. The characteristic ions of each metabolite were screened with the QQQ mass spectrometer to obtain the signal strengths. Integration and correction of chromatographic peaks was performed using Progenesis QI software (Waters Co., Milford, MA, USA). The corresponding relative metabolite contents were represented as chromatographic peak area integrals. In addition, potential metabolites were identified

using public databases including Human Metabolome Database (http://www.hmdb.ca), MassBank (http://www.massbank.jp), and Metlin (https://metlin.scripps.edu).

Data processing and analysis

Metabolites were used for hierarchical clustering analysis (HCA) and heat map analysis, which were conducted using R package, version 3.3.1. Subsequently, PCA and aoOPLS-DA were conducted using SIMCA-P14.0 software (Umetrics, Umeå, Sweden) to process data from the LC-MS/MS analysis. Significant differences between metabolites of experimental and control groups were identified using variable importance in projection (VIP) from OPLS-DA (VIP > 1). Kyoto Encyclopedia of Genes and Genomes (KEGG) database (http://www.genome.jp/kegg/) was used to identify enriched pathways of the differing metabolites.

The qRT-PCR and enzyme activity data from the three independent biological replicates were analyzed by one-way ANOVA using SPSS 19.0 (SPSS Inc., Chicago, IL, USA) for the comparison of multiple means. All data are expressed as means ± SD and significance was assumed at $p < 0.05$. Further, all the data were illustrated using GraphPad Prism 6.01 (GraphPad Software, San Diego, CA).

Results

SCD is expressed during follicular development in vivo

We performed qRT-PCR analysis to detect the expression patterns of *SCD* in the granulosa and theca layers during follicular development (Figure. 1B). The results showed that *SCD* was primarily expressed in the granulosa layer and weakly expressed in the theca layer. The *SCD* gene was upregulated in the granulosa layers of the large preovulatory follicles; expression was the highest in F1. In the prehierarchal follicles, *SCD* expression was the greatest in the 4–6 mm and 8–10 mm size categories.

SCD is expressed during GC in vitro culturing

The goose GCs were cultured in vitro for 7 d; culture medium was replaced with fresh medium every 2 d. We found that *SCD* is expressed in a time-dependent oscillation that begins on the first day of culturing (Figure. 2A). Our subsequent investigation of SCD activity, as measured by the assay kit (Figure. 2B), revealed a trend similar to that of the relative *SCD* level.

A GC cellular model of SCD function

To directly analyze the functional impact of *SCD* in GCs, we generated GCs that transiently overexpress *SCD* (referred to as GFP-SCD) and confirmed *SCD* expression by qRT-PCR (Fig. 3A). After 24, 48, and 72 h of transfection, higher expression levels of *SCD* were detected in the transfected group ($p < 0.05$) than in the GFP vector group or the empty control group. We further conducted knockdown studies using siRNA transfection, as shown in Fig. 3B. The expression of *SCD* was reduced after specific SCD-siRNA transfection compared to transfection with scrambled siRNA; the exceptions were siRNA-774, siRNA-210, and siRNA-405, all of which showed reduced *SCD* expression ($p < 0.05$) after 24, 48, and 72 h of transfection. An overexpressed *SCD* group (referred to as S), the GFP vector group (referred to as G), the control group (referred to as N), two independent siRNA groups (siRNA-210 and siRNA-470, referred to as T and F, respectively), and a scrambled siRNA group (referred to as C) were selected for further LC-MS/MS analysis.

Metabolite differences in N v. S, G v. S, C v. T, and C v. F

Based on the cell transfection efficiency in both the *SCD*-overexpressing and knockdown groups, ten million cells from each group were collected 48 h after transfection. Metabolite detection was performed using three parallel groups. A total of 333 intracellular metabolites were determined; these included amino acids, lipids, fatty acids, nucleotides, and organic acids. LC-MS/MS analysis was conducted to ensure the accuracy of the results. A complete heatmap of abundant metabolites is presented in Figure S1. As shown in Fig. 4, the principal component analysis (PCA) and orthogonal correction partial least squares discriminant analysis (OPLS-DA) score plots that we constructed using the acquired metabolomic data set revealed that the structure and quality of the data represented the close relationships among the biological replicates and the samples were distinguished by better clustering and separation between the experimental and control groups. We employed unsupervised hierarchical clustering of significantly different metabolite sets in order to determine differences between the overexpressing and knockdown groups (Fig. 5). A total of 75 metabolites showed significant differences in N v. S (41 upregulated and 34 downregulated) based on fold change analysis (VIP > 1, FC > 1.2); 50 metabolites showed significant differences in G v. S (17 upregulated and 33 downregulated); 37 showed significant differences in C v. T (14 upregulated and 23 downregulated); and 58 showed significant differences in C v. F (24 upregulated and 34 downregulated; Table S2). We arranged the 20 metabolites showing the greatest significant differences according to the $\log2^{FC}$ of each group and found that cholesterol showed the greatest change in the overexpressing group, while

pantothenol showed the greatest change in the knockdown group (Figure S2). To examine the effects of *SCD* overexpression and knockdown on the GC metabolome, we compared differences in metabolites in each group (Fig. 6). We found an overlap of 22 metabolites (7 upregulated and 10 downregulated; however Phe-Phe, N-Acetyl-5-hydroxytryptamine, 2-Aminoethanesulfonic acid, 2-(Dimethylamino)guanosine, and spermidine showed the opposite trend) between N and S and between G and S, and an overlap of 14 metabolites (6 upregulated and 8 downregulated) between C and T and between C and F.

Pathway analysis of differentially abundant metabolites

A functional analysis of pathways related to the differential abundances of metabolites was conducted using KEGG analysis. As shown in Supplementary Material Table S3, 46 of these differentially expressed metabolites were associated with 58 metabolic pathways in N v. S; 31 metabolites with 40 metabolic pathways in G v. S; 22 metabolites with 38 metabolic pathways in C v. T; and 32 metabolites with 59 metabolic pathways in C v. F. We performed topology-based pathway analysis on the top 20 pathways found in the overexpressing and knockdown groups. Figure 7 shows that SCD overexpression had a significant effect on taurine and hypotaurine metabolism; sulfur metabolism; primary bile acid biosynthesis; glycine, serine, and threonine metabolism; glutathione metabolism; and ABC transporters. Knockdown of SCD had a significant effect on purine metabolism, insulin signaling pathway, glycolysis/gluconeogenesis, galactose metabolism, the FoxO signaling pathway, amino sugar and nucleotide sugar metabolism, and the AGE-RAGE signaling pathway in diabetic complications. Both the overexpressing and knockdown groups were metabolically enriched in 10 lipid-related pathways (Table 1); the 25 other enriched lipid-related metabolic pathways of overexpressing or knockdown groups are shown in Table S4. Of these, Tyrosine metabolism, Arginine biosynthesis/ D-Arginine and D-ornithine metabolism, alpha-Linolenic acid metabolism, Taurine and hypotaurine metabolism were enriched in the metabolic pathway that was specifically enriched in the overexpressed group. Glycolysis/gluconeogenesis, insulin signaling pathway, and lysosome were enriched in the metabolic pathway that was specifically enriched in the knockdown group.

Table 1
Metabolic pathways and significantly different metabolites were associated with lipid metabolism and enriched in both the overexpressed and the knockdown groups.

Pathway	N v. S	G v. S	C v. T	C v. F	lipid-related functions reported	Reference
Steroid hormone biosynthesis/ Steroid biosynthesis	Cholesterol	Cholesterol	Androsterone/ Vitamin D3	Androsterone	Steroid hormones are essential regulators of a vast number of physiological processes.	[31]
]Galactose metabolism	UDP-glucose	D-Sorbitol; Dulcitol	D-Glucose; D-Sorbitol	D-Glucose; Myoinositol	galactose exerts primarily suppressive effects of ovarian follicle number and steroid secretion by direct actions on the ovary	[32]
Tryptophan metabolism	N-Acetyl-5-Hydroxytryptamine; Anthranilic acid	N-Acetyl-5-Hydroxytryptamine	Succinic Acid	Epinephrine	molecular modeling studies suggested favorable stacking interactions between cholesterol and tryptophan where the face of the complex ring system of cholesterol and the indole ring of tryptophan build the interaction interface	[33]
Sulfur metabolism	L-Cysteine; 2-Aminoethanesulfonic Acid	2-Aminoethanesulfonic Acid; L-Homoserine	Succinic Acid	L-Homoserine	Recently, increasing attention has been paid to the role of sulfur amino acids in regulating lipid metabolism.	[34]
Cysteine and methionine metabolism	L-Cysteine; S-Sulfo-L-Cysteine; L-Alanine; Glutathione Reducedform; S-(5-Adenosy)-L-Homocysteine	L-Homoserine; L-Cystine	S-Sulfo-L-Cysteine	L-Homoserine; S-(5-Adenosy)-L-Homocysteine	Much attention has been recently focused on the effects of Methionine restriction and Cysteine on metabolic health, especially lipid metabolism,	[35, 36]
pyrimidine metabolism	Uridine 5-Monophosphate; UDP-glucose	B-Pseudouridine	Cytidine; 2-Deoxyribose 1-Phosphate	2-Deoxyribose 1-Phosphate	Given the link between pyrimidine metabolism and liver lipid accumulation, there is a potential for the use of nucleosides and nucleoside analogs in the treatment of fatty liver condition.	[37]
Pantothenate and CoA biosynthesis	Pantothenate; L-Cysteine	Pantothenol	Pantothenol	Pantothenol	Pantothenate forms the core of CoA and is a precursor to acyl carrier protein (ACP), making it essential in both energy and lipid metabolism.	[38]

Pathway	N v. S	G v. S	C v. T	C v. F	lipid-related functions reported	Reference
Biosynthesis of amino acids	Anthranilic acid; Glycine; S-Sulfo-L-Cysteine; S-(5-Adenosy)-L-Homocysteine; L-Threonine; L-Alanine; L-Cysteine; L-Ornithine; L-Isoleucine	L-Ornithine; L-Homoserine; L-Threonine; Shikimic Acid	S-Sulfo-L-Cysteine	L-Homoserine; Glycine; L-Asparagine Anhydrous; S-(5-Adenosy)-L-Homocysteine	amino acids were distributed in a lipid bilayer	[39]
ABC transporters	2-Aminoethanesulfonic Acid; Spermidine; proline betaine; Glycine; Betaine; Glutathione Reducedform; L-Ornithine; L-Isoleucine; Biotin; Choline; L-Threonine; L-Alanine; Inosine	Betaine; D-Sorbitol; Inosine; L-Cystine; L-Threonine; L-Ornithine; D-Mannitol; Spermidine; Guanosine; proline betaine; 2-Aminoethanesulfonic Acid; Xanthosine	D-Sorbitol; Xanthosine; Glycerol 3-phosphate; D-Glucose; Cytidine	Biotin; Myoinositol; Spermidine; Glycerol 3-phosphate; Glycine; Inosine; Guanosine; D-Glucose	ATP binding cassette (ABC) transporter proteins are thought to facilitate the ATP-dependent translocation of lipids or lipid-related compounds, such substrates include cholesterol, plant sterols, bile acids, phospholipids and sphingolipids.	[40]
Neuroactive ligand-receptor interaction	2-Aminoethanesulfonic Acid; L-Thyroxine; Glycine	2-Aminoethanesulfonic Acid; Norepinephrine	Adenosine 5'-Diphosphate	Adenosine 5'-Diphosphate; Epinephrine; Glycine	Modulation of neurotransmitter receptors by lipids occurs at multiple levels, affecting a wide span of activities including their trafficking, sorting, stability, residence lifetime at the cell surface, endocytosis, and recycling, among other important functional properties at the synapse.	[41]

Discussion

The expression of SCD is tissue-specific and sex-dependent dependent. Previous studies in chickens revealed that the second-highest *SCD* expression occurs in the ovaries [42]. This could be due to differences in fat deposition and/or levels of hormones, particularly sex hormones, within tissues (e.g., estrogen, androgen, and GH) [43]. In this study, the result showed that SCD expression was significantly higher in the granulosa than in the theca layer (Fig. 1B). We therefore speculated that the function of SCD in goose GCs is closely to related follicular development. In addition, we demonstrated that the expression levels of *SCD* increase during follicular recruitment and selection processes, reaching a peak during ovulation (Fig. 1B). Many developing follicles undergo atresia as they advance toward ovulation, except for those undergoing the recruitment and selection processes. It is well known that GC death via apoptosis is the main cause of atresia [44]. Our results suggest the vital role that *SCD* plays in inhibiting GC apoptosis. Emerging evidence suggests a crucial role for *SCD* in the regulation of programmed cell death and lipid-mediated cytotoxicity [45]. The antiapoptotic effect of *SCD* can likely be attributed to the conversion of excess toxic SFAs into relatively harmless MUFAs by the desaturase, which regulates the ratio of SFAs available for modulating membrane fluidity and signal transduction [46].

The intracellular concentration of SCD fluctuates widely in response to complex and often competing hormonal and dietary factors. A combination of transcriptional regulation and rapid protein degradation produces transient elevations of SCD activity in response to physiological demands [47]. We found that *SCD* was expressed in a time-dependent dynamic oscillation during the seven days of primary in vitro GC culture; this trend was similar to that observed for SCD activity (Fig. 2). The observation that changes in mRNA expression are paralleled by changes in activity of the corresponding enzyme allows us to conclude that the change in enzyme activity is due to altered gene expression. Experiments on the liver support the idea that the *SCD* mRNA levels are directly indicative of the desaturase activity; modification of SCD activity in liver cells can be achieved by modifying the *SCD* mRNA level [48]. This enzymatic reaction plays a critical role in directing the cell towards either lipid synthesis or oxidation, and produces diverse effects on cellular function [49]. We hypothesize that

SCD is a primary regulator in the process of lipid homeostasis in goose GCs. Studies using the CHO cell line confirm this view. SCD activity was shown to increase when CHO cells were incubated with lipid-depleted media; however, when the medium was supplemented with cholesterol, the desaturase activity was reduced [50].

This study revealed the metabolites and the metabolic pathways in SCD-overexpressing and -knockdown GCs based on a metabolomic analysis. Our study showed that ten lipid-related pathways were enriched in overexpressed and knockdown SCD groups; lipid-related functions are shown in Table 1. The results reported here provide new evidence that SCD functions in the regulation of lipid metabolism processes of goose follicle development. Overexpression of SCD enhanced the intracellular level of cholesterol, which is involved in the steroid hormone biosynthesis/steroid biosynthesis pathway (Table 1 and Figure S2). We speculate that the overexpression of SCD may facilitate the synthesis and subsequent esterification of cholesterol into lipid droplets (LDs) in goose GCs. Our recently published study demonstrated that vital miRNA–mRNA interactions related to lipid regulation, including LD formation, occur during goose follicular selection [19]. Furthermore, our research indicated that LD accumulation capacity depends on the stage of follicle development, with the highest lipid content found in F1 GCs (not publish). The in vivo results of this study similarly showed peak SCD expression in F1 granulosa layers (Fig. 1). These findings support the possibility that a similar mechanism transpires in mammals, for which lipid metabolism is assumed to be essential for follicular development and oocyte energy supply [51, 52]. In addition, while the knockdown of SCD maximally enhanced the content of pantothenol, which is a component of pantothenate and coenzyme A (CoA), SCD overexpression decreased the levels of pantothenol and pantothenate (Table 1 and Figure S2). Based on this finding, we postulate for the first time that pantothenate and CoA participate in goose follicle lipid metabolism. Pantothenate forms the core of CoA, which occurs in sequestered pools in eukaryotic cells and plays important roles in lipid synthesis, microsomal fatty acid oxidation, protein modifications, and membrane trafficking [53, 54]. Cholesterol and pantothenol or pantothenate could potentially serve as metabolite biomarkers; the pathways underlying these associations are shown in Fig. 8. An important avenue of future study entails research into the potential functions of SCD in lipid metabolism of goose GCs.

Conclusions

Our findings point to the vital role that SCD during follicular development, which from a comparison of *SCD*-overexpressing cells with *SCD*-knockdown cells, details the lipid metabolism-related pathways that are affected by both of these conditions. And confirmed cholesterol and pantothenol / pantothenate as potential metabolite biomarkers to research the lipid metabolism of *SCD* in goose GCs.This understanding should shed light on mechanisms of lipid metabolism in avian follicular development.

Abbreviations

CoA coenzyme A

DNL de novo lipogenesis

GC granulosa cell

HCA hierarchical clustering analysis

KEGG Kyoto Encyclopedia of Genes and Genomes

LIT linear ion trap

LC-ESI-MS/MS liquid chromatography-electrospray ionization-tandem mass spectrometry

LC-MS/MS liquid chromatography-tandem mass spectrometry

MUFA monounsaturated fatty acid

MRM multiple reaction monitoring

NC negative control

OPLS-DA orthogonal correction partial least squares discriminant analysis

PUFA polyunsaturated fatty acid

PCA principal component analysis

QC quality control

qRT-PCR quantitative real-time PCR

SFA saturated fatty acid

siRNA small interfering RNA

SCD stearoyl-CoA desaturase

QQQ triple quadrupole

VIP variable importance in projection

LD lipid droplet

Declarations

Ethics approval and consent to participate

The animal experiment was reviewed and approved by the Committee of the School of Farm Animal Genetic Resources Exploration and Innovation Key Laboratory, College of Animal Science and Technology, Sichuan Agricultural University, and was performed in accordance with the Regulations for the Administration of Affairs Concerning Experimental Animals (China 1988). This study was conducted in accordance with the requirements of the Beijing Animal Welfare Committee. All efforts were made to minimize animal suffering.

Consent for publication

Not applicable.

Availability of data and materials

All data generated or analyzed during this study are available from the corresponding author upon reasonable request.

Competing interests

The authors declare that they have no competing interests.

Funding

This study was supported by a grant from the National Natural Science Foundation of China (No. 31672424 and 035Z2425), the China Agricultural Research System (No. CARS-42-4), the Open Fund of Farm Animal Genetic Resources Exploration and Innovation Key Laboratory of Sichuan Province (SNDK-KF-201802), the Project of National Science and Technology Plan for the Rural Development in China (No. 2015BAD03B06), and the Key Technology Support Program of Sichuan Province (No. 2016NYZ0044).

Authors' contributions

Data curation and review and formal analysis; X.Y., S.Q.H.; Conceptualization and Supervision: L.L., H.H.; Writing-original draft preparation: X.Y.; Review and editing: H.H.L., J.W.W. All authors have read and agreed to the published version of the manuscript.

Acknowledgements

Not applicable.

Author information

Affiliations

Farm Animal Genetic Resources Exploration and Innovation Key Laboratory of Sichuan Province, College of Animal Science and Technology, Sichuan Agricultural University, Chengdu, P. R. 611130, China

Xin Yuan, Shenqiang Hu, Liang Li, Hehe Liu, Hua He and Jiwen Wang

Corresponding author

Correspondence to Jiwen Wang

References

1. Bai, Y., Mccoy, J.G., Levin, E.J., Sobrado, P., Rajashankar, K.R., Fox, B.G., and Zhou, M. (2015). X-ray structure of a mammalian stearoyl-CoA desaturase. Nature *524, 252-256.* DOI 10.1038/nature14549
2. Wu, X., Zou, X., Chang, Q., Zhang, Y., Li, Y., Zhang, L., Huang, J., and Liang, B. (2013). The evolutionary pattern and the regulation of stearoyl-CoA desaturase genes. BioMed. Res. Int. 856521-856521. DOI 10.1155/2013/856521
3. Alarcon, G.D.J., Roco, J., Medina, A., Van Nieuwenhove, C., Medina, M., and Jerez, S. (2016). Stearoyl-CoA desaturase indexes and n-6/n-3 fatty acids ratio as biomarkers of cardiometabolic risk factors in normal-weight rabbits fed high fat diets. J. Biomed. Sci. *23*, 13-13. DOI 10.1186/s12929-016-0235-6
4. Kamal, S., Saleem, A., Rehman, S., Bibi, I., and Iqbal, H.M.N. (2018). Protein engineering: Regulatory perspectives of stearoyl CoA desaturase. Int. J. Bio. Macromol. 692-699. DOI 10.1016/j.ijbiomac.2018.03.171
5. Castro, L.F.C., Wilson, J.M., Goncalves, O., Galanteoliveira, S., Rocha, E., and Cunha, I. (2011). The evolutionary history of the stearoyl-CoA desaturase gene family in vertebrates. BMC. Evol. Biol. *11*, 132-132. DOI 10.1186/1471-2148-11-132
6. Aljohani, A.M., Syed, D.N., Ntambi, J.M. (2017). Insights into Stearoyl-CoA Desaturase-1 Regulation of Systemic Metabolism. Trends. Endocrin. Met. *28*, 831-842. DOI 10.1016/j.tem.2017.10.003
7. Park, W.J. (2018). Polyunsaturated Fatty Acid Metabolism || The Biochemistry and Regulation of Fatty Acid Desaturases in Animals. Academic Press and AOCS Press, pp. 87-100 DOI 10.1016/B978-0-12-811230-4.00005-3
8. Shen, J., Gang, W., Tsai, A.L., and Ming, Z. (2018). Structure and Function of Mammalian Stearoyl-COA Desaturase. Biophys. J. *114.* DOI 10.1016/j.bpj.2017.11.2361
9. Frigolet, M.E., and Gutierrezaguilar, R. (2017). The Role of the Novel Lipokine Palmitoleic Acid in Health and Disease. Adv. Nutr*. 8.* DOI 10.3945/an.115.011130
10. Ran, H., Zhu, Y., Deng, R., Zhang, Q., Liu, X., Feng, M., Zhong, J., Lin, S., Tong, X., Su, Q. (2018). Stearoyl-CoA desaturase-1 promotes colorectal cancer metastasis in response to glucose by suppressing PTEN. J. Exp. Clin. Canc. Res. *37, 1-15.* DOI 10.1186/s13046-018-0711-9
11. Zhao, J., Zhi, Z., Wang, C., Xing, H., Song, G., Yu, X., Zhu, Y., Wang, X., Zhang, X., and Di, Y. (2017). Exogenous lipids promote the growth of breast cancer cells via CD36. Oncol. Rep. *38, 2105-2115.* DOI 10.3892/or.2017.5864
12. Zhang, Yong-Mei (2016). Biochemistry of Lipids, Lipoproteins and Membranes || Fatty Acid and Phospholipid Biosynthesis in Prokaryotes. pp. 73-112 DOI 10.1016/B978-0-444-63438-2.00003-1
13. Uzbekova, S., Elis, S., Teixeiragomes, A., Desmarchais, A., Maillard, V., and Labas, V. (2015). MALDI Mass Spectrometry Imaging of Lipids and Gene Expression Reveals Differences in Fatty Acid Metabolism between Follicular Compartments in Porcine Ovaries. Biology *4, 216-236.* DOI 10.3390/biology4010216
14. Vireque, A.A., Tata, A., Belaz, K.R.A., Grázia, J.O.G.V., Santos, F.N., Arnold, D.R., Basso, A.C., Eberlin, M.N., Silva-De-Sá, M.F., and Ferriani, R.A., Rosaesilva, A.C.G.D.S. (2017). MALDI mass spectrometry reveals that cumulus cells modulate the lipid profile of in vitro matured bovine oocytes. Syst. Bio. Reprod. Med. *63, 86-99.* DOI 10.1080/19396368.2017.1289279
15. Elis, S., Desmarchais, A., Maillard, V., Uzbekova, S., Monget, P., and Dupont, J. (2015). Cell proliferation and progesterone synthesis depend on lipid metabolism in bovine granulosa cells. Theriogenology *83*, 840-853. DOI 10.1016/j.theriogenology.2014.11.019
16. Campbell, B.K., Onions, V., Kendall, N.R., Guo, L., and Scaramuzzi, R.J. (2010b). The effect of monosaccharide sugars and pyruvate on the differentiation and metabolism of sheep granulosa cells in vitro. Reproduction *140,* 541-550. DOI 10.1530/REP-10-0146
17. Hu, W., and Qiao, J. (2011). Expression and regulation of adipocyte fatty acid binding protein in granulosa cells and its relation with clinical characteristics of polycystic ovary syndrome. Endocrine *40, 196-202.* DOI 10.1007/s12020-011-9495-9
18. Wen, R.; Gan, X.; Hu, S.Q.; Gao, S.Y., Deng, Y., Qiu, J.M., Sun, W.Q., Li, L., Han, C.C., Hu, J.W., Wang, J.W (2018). Evidence for the existence of de novo lipogenesis in goose granulosa cells.Poultry. Sci. *98*, 1023-1030. DOI 10.3382/ps/pey400
19. Li, Q., Hu, S., Wang, Y., Deng, Y., Yang, S., Hu, J., Li, L., and Wang, J. (2019). mRNA and miRNA Transcriptome Profiling of Granulosa and Theca Layers From Geese Ovarian Follicles Reveals the Crucial Pathways and Interaction Networks for Regulation of Follicle Selection.

Front. Genet. *10.* DOI 10.3389/fgene.2019.00988

20. Suttonmcdowall, M.L., Gilchrist, R.B., and Thompson, J.G. (2010). The pivotal role of glucose metabolism in determining oocyte developmental competence. Reproduction *139,* 685-695. DOI 10.1530/REP-09-0345
21. Bednarski, T., Olichwier, A., Opasinska, A., Pyrkowska, A., Gan, A., Ntambi, J.M., and Dobrzyn, P. (2016). Stearoyl-CoA desaturase 1 deficiency reduces lipid accumulation in the heart by activating lipolysis independently of peroxisome proliferator-activated receptor α. Biochim. Biophys. Acta. *1861*, 2029-2037. DOI 10.1016/j.bbalip.2016.10.005
22. Dobrzyn, P., Dobrzyn, A., Miyazaki, M., Cohen, P., Asilmaz, E., Hardie, D.G., Friedman, J.M., and Ntambi, J.M. (2004). Stearoyl-CoA desaturase 1 deficiency increases fatty acid oxidation by activating AMP-activated protein kinase in liver. P. Nati. Acad. Sci. USA. *101, 6409-6414.* DOI 10.1073/pnas.0401627101
23. Phillips, R.W., Johnson, R.G., and Moyer, R.T. (1948). China's Goose Industry. World. Poultry. Sci. J. *4, 34-35.* DOI 10.1079/WPS19480010
24. Johnson, A.L. (2011). Chapter 3 – Organization and Functional Dynamics of the Avian Ovary. Hormones & Reproduction of Vertebrates *40*, 71-90. DOI 10.1002/3527608494.ch2
25. Johnson, P.A. (2012). Follicle Selection in the Avian Ovary. Reprod. Domest. Anim. *283-287.* DOI 10.1111/j.1439-0531.2012.02087.x
26. Trivedi, D.K., Hollywood, K.A., and Goodacre, R. (2017). Metabolomics for the masses: The future of metabolomics in a personalized world. New Horizons in Translational Medicine *3, 294-305.* DOI 10.1016/j.nhtm.2017.06.001
27. Nicholson, J.K., and Lindon, J.C. (2008). Systems biology: Metabonomics. Nature *455*, 1054-6. DOI 10.1038/4551054a. DOI 10.1038/4551054a
28. Gilbert, A. (1971). The Ovary. physiology & biochemistry of the domestic fowl Physiology & Biochemistry of the Domestic Fowl, *3*.
29. Gilbert, A., Evans, A., Perry, M., and Davidson, M. (1977). A method for separating the granulosa cells, the basal lamina and the theca of the preovulatory ovarian follicle of the domestic fowl (Gallus domesticus). Journal of Reproduction and Fertility J. Reprod. Fertil. *50*, 179-181 DOI 10.1530/jrf.0.0500179
30. Livak, K.J., and Schmittgen, T.D. (2000). Analysis of Relative Gene Expression Data Using Real-Time Quantitative PCR and the $2^{-\triangle\triangle Ct}$ Method. *Methods 25, 402-408.* DOI 10.1006/meth.2001.1262
31. Lucki, N.C., and Sewer, M.B. (2008). Multiple Roles for Sphingolipids in Steroid Hormone Biosynthesis. Sub-cellular biochemistry *49, 387-412.* DOI 10.1007/978-1-4020-8831-5_15
32. Campbell, B.K., Kendall, N.R., Onions, V., and Scaramuzzi, R.J. (2010a). The effect of systemic and ovarian infusion of glucose, galactose and fructose on ovarian function in sheep. Reproduction *140*, 721-732. DOI 10.1530/REP-10-0185
33. Holt, A., De Almeida, R.F.M., Nyholm, T.K.M., Loura, L.M.S., Daily, A.E., Staffhorst, R.W.H.M., Rijkers, D.T.S., Koeppe, R.E., Prieto, M., and Killian, J.A. (2008). Is there a preferential interaction between cholesterol and tryptophan residues in membrane proteins. Biochemistry *47*, 2638-2649. DOI 10.1021/bi702235k
34. Lee, J., Jung, S., Kim, N., Shin, M.J., Ryu, D.H., and Hwang, G. (2017). Myocardial metabolic alterations in

mice with diet-induced atherosclerosis: linking sulfur amino acid and lipid metabolism. Sci. Rep. *7, 13597.* DOI 10.1038/s41598-017-13991-z

35. Carter, R.N., and Morton, N.M. (2015). Cysteine and hydrogen sulphide in the regulation of metabolism: insights from genetics and pharmacology. J. Pathol. *238,* 321-332. DOI 10.1002/path.4659
36. Zhou, X., He, L., Wan, D., Yang, H., Yao, K., Wu, G., Wu, X., and Yin, Y. (2016). Methionine restriction on lipid metabolism and its possible mechanisms. Amino Acids *48, 1533-1540.* DOI 10.1007/s00726-016-2247-7
37. Le, T.T., Ziemba, A., Urasaki, Y., Hayes, E., Brotman, S., and Pizzorno, G. (2013). Disruption of uridine homeostasis links liver pyrimidine metabolism to lipid accumulation. J. Lipid Res. *54, 1044-1057.* DOI 10.1194/jlr.M034249
38. Miller, C.N., LoVullo, E.D., Kijek, T.M., Fuller, J.R., Brunton, J.C., Steele, S.P., Taft-Benz, S.A., Richardson, A.R., and Kawula, T.H (2013). PanG, a New Ketopantoate Reductase Involved in Pantothenate Synthesis. J. Bacteriol. *195, 965-976.* DOI 10.1128/JB.01740-12
39. Maccallum, J.L., Bennett, W.F.D., and Tieleman, D.P (2008). Distribution of Amino Acids in a Lipid Bilayer from Computer Simulations. Biophys. J. *94, 3393-3404.* DOI 10.1529/biophysj.107.112805
40. Tarling, E.J., Vallim, T.Q.D.A., Edwards, P.A. (2013). Metabolism, Role of ABC transporters in lipid transport and human disease. Trend. Endocrin. Met. *24, 342-350.* DOI 10.1016/j.tem.2013.01.006

41. Borroni, M.V., Vallés, A.S., and Barrantes, F.J. (2016). The lipid habitats of neurotransmitter receptors in brain. Bba-Biomembranes *1858, 2662-2670.* DOI 10.1016/j.bbamem.2016.07.005
42. Dridi, S., Taouis, M., Gertler, A., Decuypere, E., and Buyse, J. (2007). The regulation of stearoyl-CoA desaturase gene expression is tissue specific in chickens. J. Endocrin. *192, 229-236.* DOI 10.1677/JOE-06-0070
43. Mauvoisin, D., and Mounier, C. (2011). Hormonal and nutritional regulation of SCD1 gene expression. Biochimie. *93, 0-86.* DOI 10.1016/j.biochi.2010.08.001
44. Matsuda, F., Inoue, N., Manabe, N., Ohkura, S. (2012). Follicular Growth and Atresia in Mammalian Ovaries: Regulation by Survival and Death of Granulosa Cells. J. Reprod. Develop. *58, 44-50.* DOI 10.1262/jrd.2011-012
45. Tesfay, L., Paul, B.T., Konstorum, A., Deng, Z., and Research, S.V. (2019). Steroyl-CoA Desaturase 1 (SCD1) protects ovarian cancer cells from ferroptotic cell death. Cancer. Res. *79,* canres.0369.2019. DOI 10.1158/0008-5472.CAN-19-0369
46. Igal, R.A. (2016). Stearoyl CoA desaturase-1: New insights into a central regulator of cancer metabolism. Bba-mol. Cell. Biol. L. *1861, 1865-1880.* DOI 10.1016/j.bbalip.2016.09.009
47. Koeberle, A., Loser, K., and Thurmer, M. (2016). Stearoyl-CoA desaturase-1 and adaptive stress signaling. Bba-mol. Cell. Biol. L. *1861, 1719-1726.* DOI 10.1016/j.bbalip.2016.08.009
48. Diot, C., Lefevre, P., Herve, C., Belloir, B., Narce, M., Damon, M., Poisson, J., Mallard, J., Douaire, M. (2000). Stearoyl-CoA desaturase 1 coding sequences and antisense RNA affect lipid secretion in transfected chicken LMH hepatoma cells. Arch. Biochem. Biophys. *380*, 0-250. DOI 10.1006/abbi.2000.1945
49. Flowers, M.T., and Ntambi, J.M. (2008). Role of stearoyl-coenzyme A desaturase in regulating lipid metabolism. Curr. Opin. Lipidol. *19*, 248-256. DOI 10.1097/MOL.0b013e3282f9b54d
50. Chin, J., and Chang, T.Y. (1982). Further characterization of a Chinese hamster ovary cell mutant requiring cholesterol and unsaturated fatty acid for growth. Biochemistry *21*, 3196-3202. DOI 10.1021/bi00256a025
51. Dunning, K.R., Russell, D.L., and Robker, R.L. (2014). Lipids and oocyte developmental competence: the role of fatty acids and β-oxidation. Reproduction *148*. DOI 10.1530/REP-13-0251
52. Prates, E.G., Nunes, J.T., and Pereira, R.M. (2014). A Role of Lipid Metabolism during Cumulus-Oocyte Complex Maturation: Impact of Lipid Modulators to Improve Embryo Production. Mediat. Inflamm. *692067-692067.* DOI 10.1155/2014/692067
53. Leonardi, R., Zhang, Y.M., Rock, C.O., and Jackowski, S. (2005). Coenzyme A: Back in action. Lipid. Res. *44, 125-153.* DOI 10.1016/j.plipres.2005.04.001
54. Dansie, L.E., Reeves, S., Miller, K., Zano, S.P., Frank, M., Pate, C., Wang, J., and Jackowski, S. (2014). Physiological roles of the pantothenate kinases. Biochem. Soc. T. *42*, 1033-1036. DOI 10.1042/bst20140096

Figures

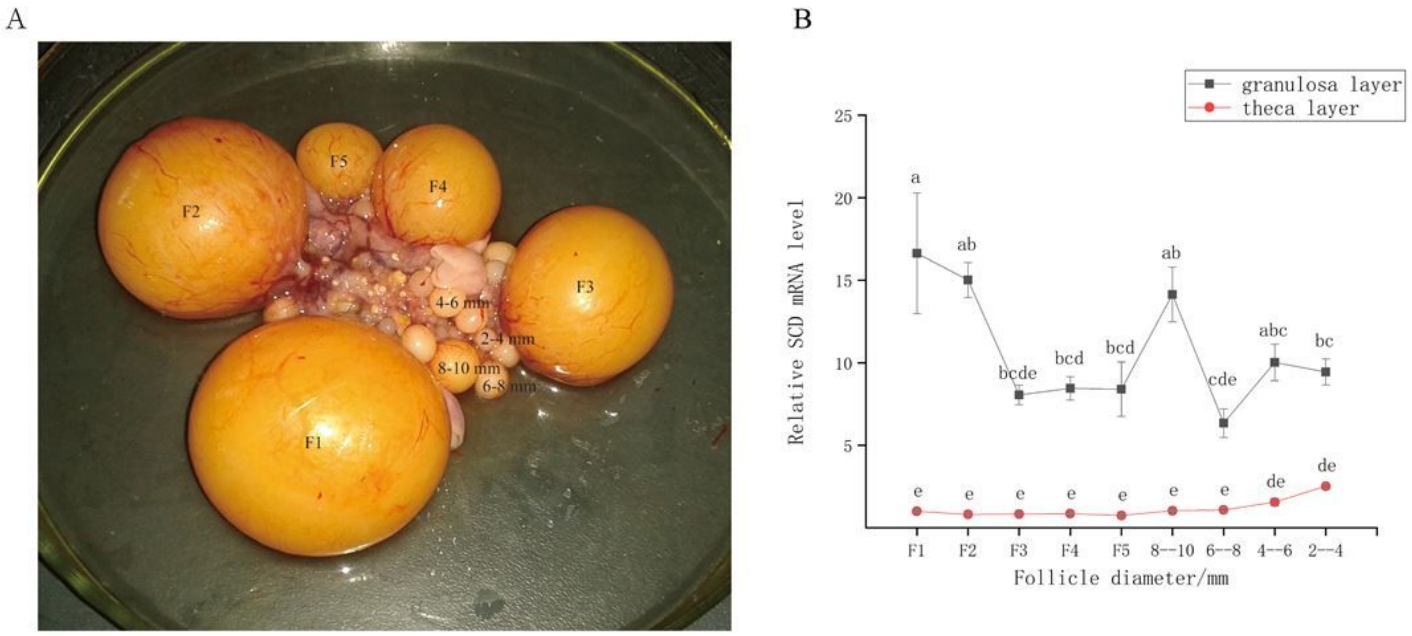

Figure 1

(A) The goose ovary contains a hierarchy of large preovulatory follicles and a small cohort of prehierarchal follicles. (B) Relative expression level of SCD in granulosa layer and theca layer during follicle development in vivo. The dataare represented as the mean ± SD (n=3), the data were analyzed by ANOVA and Tukey's test. The lowercase letter indicate significant differences between different GC layers and TC layers (P<0.05).

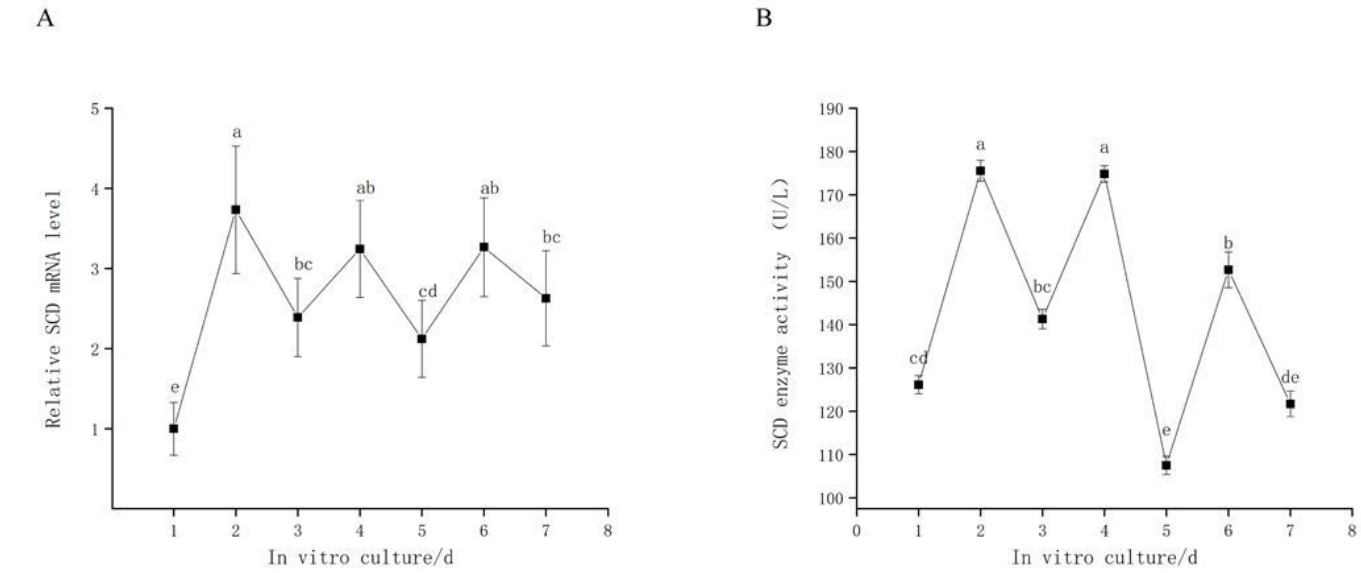

Figure 2

Relative expression level of SCD in goose GCs were cultured in vitro for 7 days. The data are represented as the mean ± SD (n=3), the data were analyzed by ANOVA and Tukey's test. The lowercase letter indicate significant differences in cultured goose GCs for 7 days in vitro (P<0.05). (B) SCD enzyme activity.

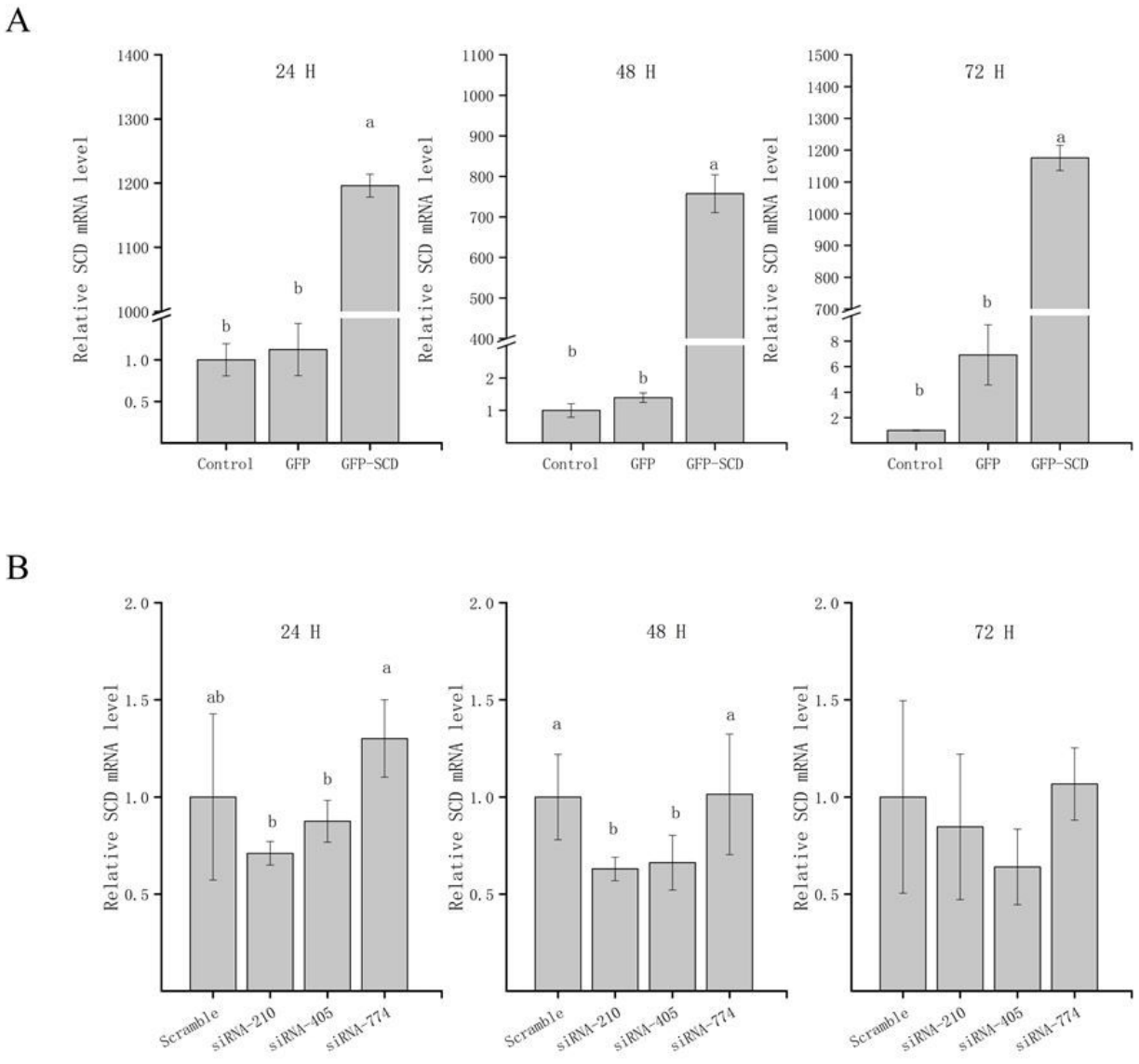

Figure 3

The detection of SCD transfection efficiency. (A) Overexpress-transfected cells were collected at the indicated time points after transfection for qRT-PCR analyses (B) siRNA-transfected cells were collected at the indicated time points after transfection for qRT-PCR analyses. The data are represented as the mean ± SD (n=3), the data were analyzed by ANOVA and Tukey's test. The lowercase letter indicate significant differences between experimental groups and control groups (P<0.05).

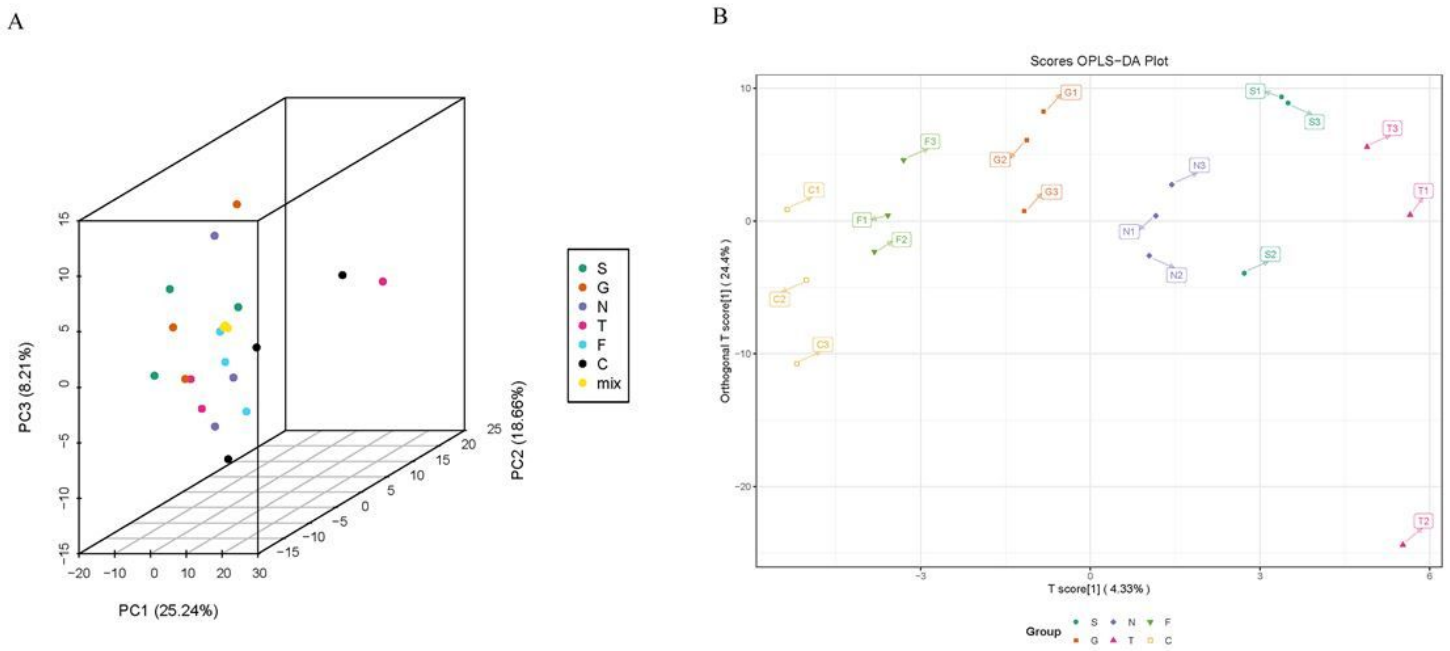

Figure 4

(A) Metabolic differences in GCs cellular model is highlighted in the Principal component analysis (PCA) score plot. An overexpressed SCD group is denoted P, GFP group is denoted P and the control group is denoted N; a siRNA-210 group is denoted T, siRNA-470 group is denoted F and scrambled siRNA group is denoted C. The scores plot shows the first three principal components, where PC1 accounts for 25.24% of the total spectral variance, PC2 accounts for 18.66% of the total spectral variance and PC3 accounts for 8.21% of the total spectral variance. (B) Orthogonal correction partial least squares discriminant analysis (OPLS-DA) of the metabolites from each group. PCA and OPLS-DA models demonstrating a separation between each group.

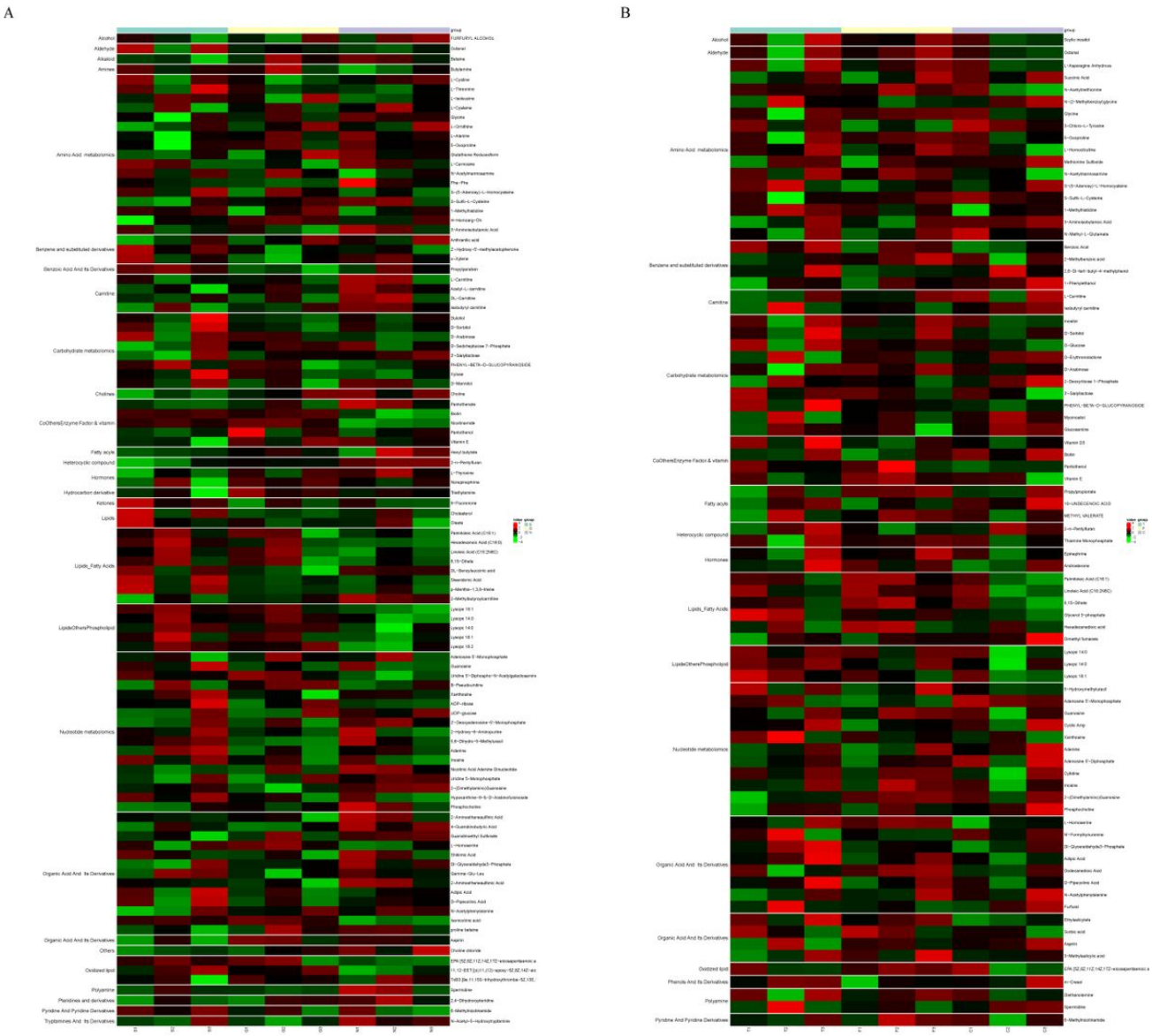

Figure 5

(A) Heat map from the hierarchical clustering of differentially metabolites in overexpress SCD group and control group. (B) Heat map from the hierarchical clustering of differentially metabolites in knockdown group and control group. The scaled expression by row (metabolites) is shown as a heat map and is reordered by a hierarchical clustering analysis (Pearson's distance and Ward's method) on both rows and columns. Significant differentially metabolites between overexpress group and knockdown group were identified with cutoff values of a VIP 1, FC 1.2. The colour scale indicates the relative amounts of metabolites: red, higher levels; green, lower levels; black, unchanged.

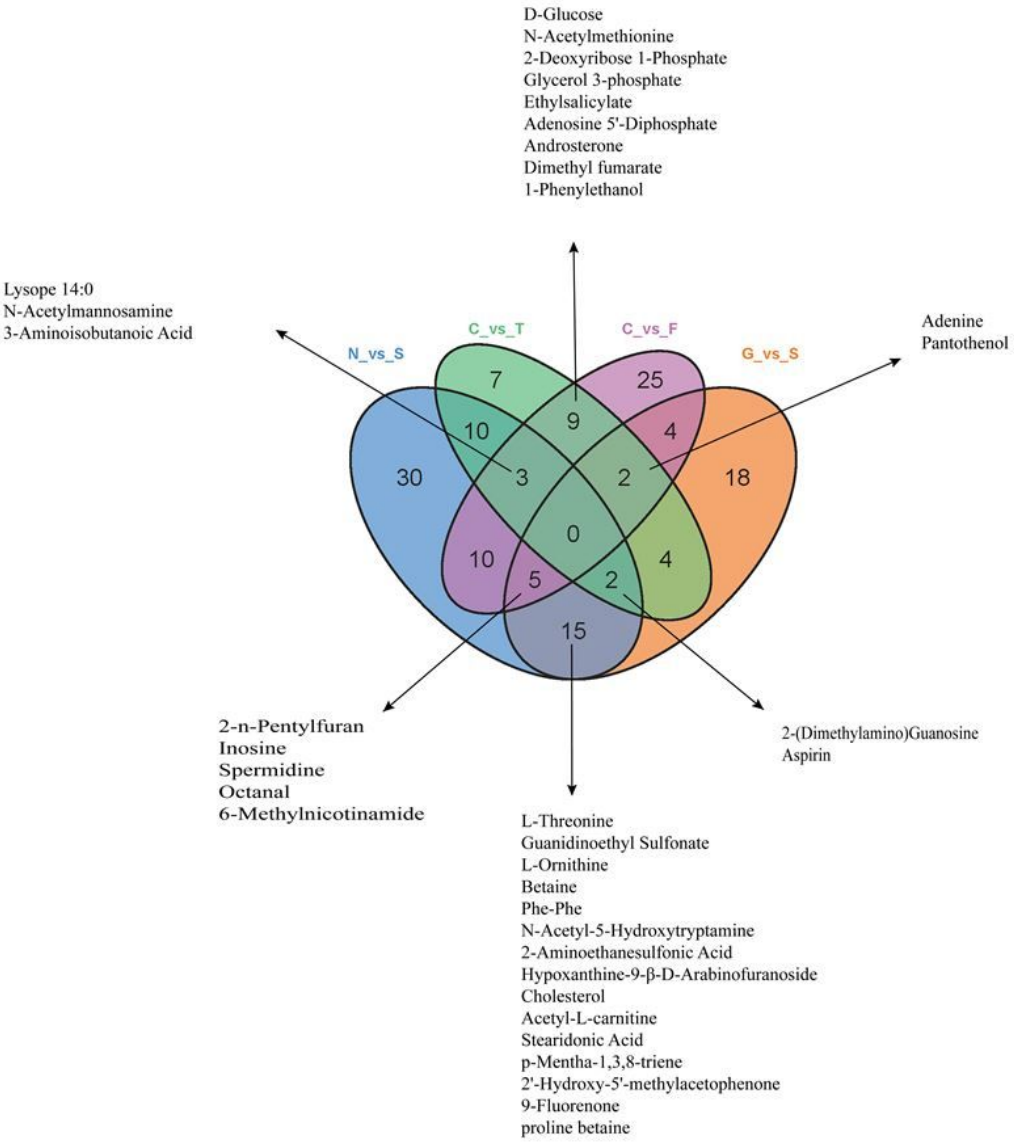

Figure 6

Venn diagram of overlapping and unique of metabolites altered in each group. A total of 22 metabolites were overlap between N v. S and G v. S; A total of 14 metabolites overlap between C v. T and C v. F (Table S2).

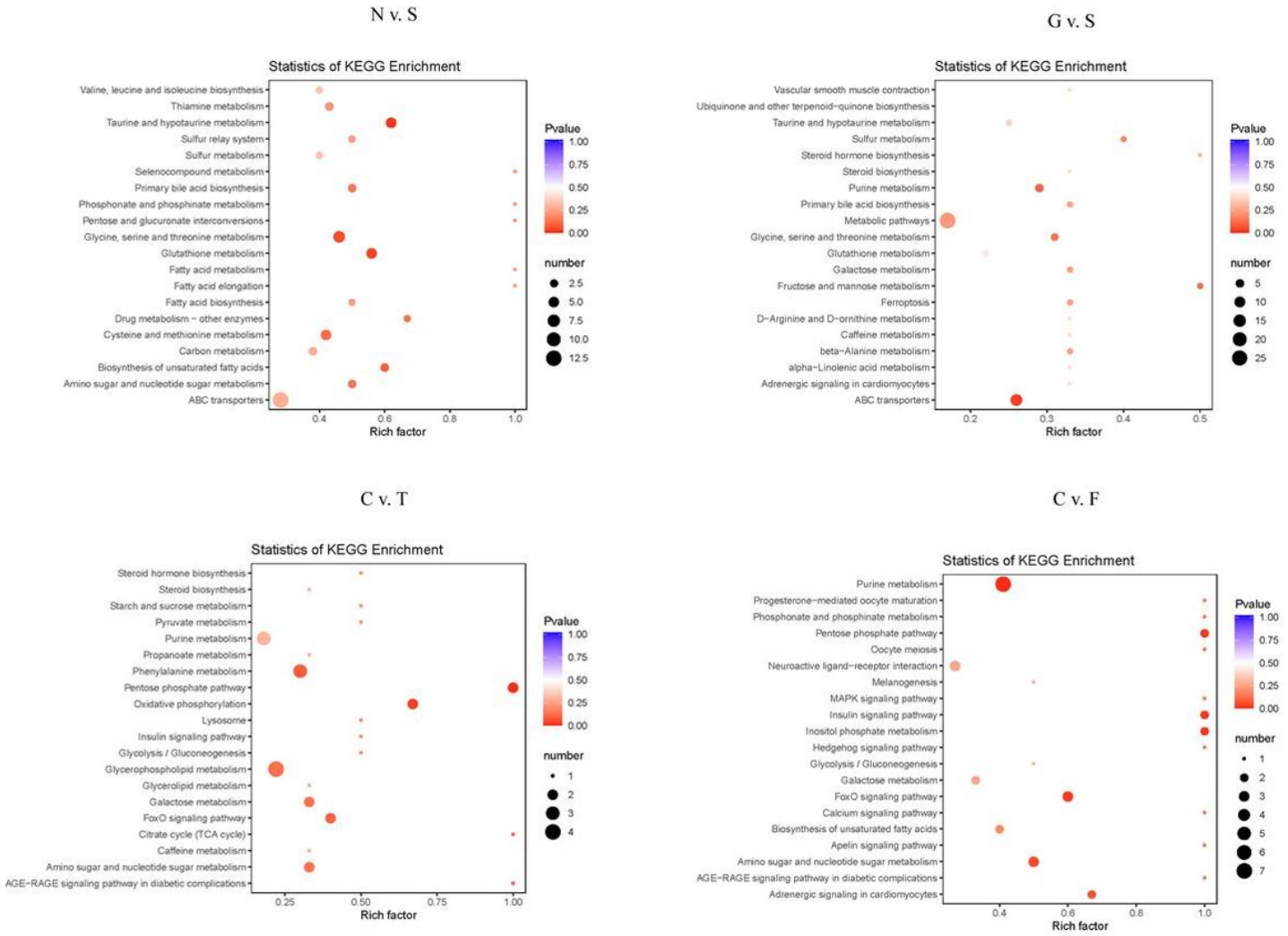

Figure 7

Topology analysis of metabolic pathways identified in the GCs of goose overexpress or knockdown SCD. Advanced bubble chart shows the enrichment of differentially abundant metabolites in pathways. The x-axis represents the rich factor (rich factor = number of different metabolites enriched in the pathway/number of all metabolites in the background metabolites set). The y-axis represents represent the enriched pathways. Size of the bubble represent the number of different abundant metabolites enriched in the pathway, and the colour represents enrichment significance.

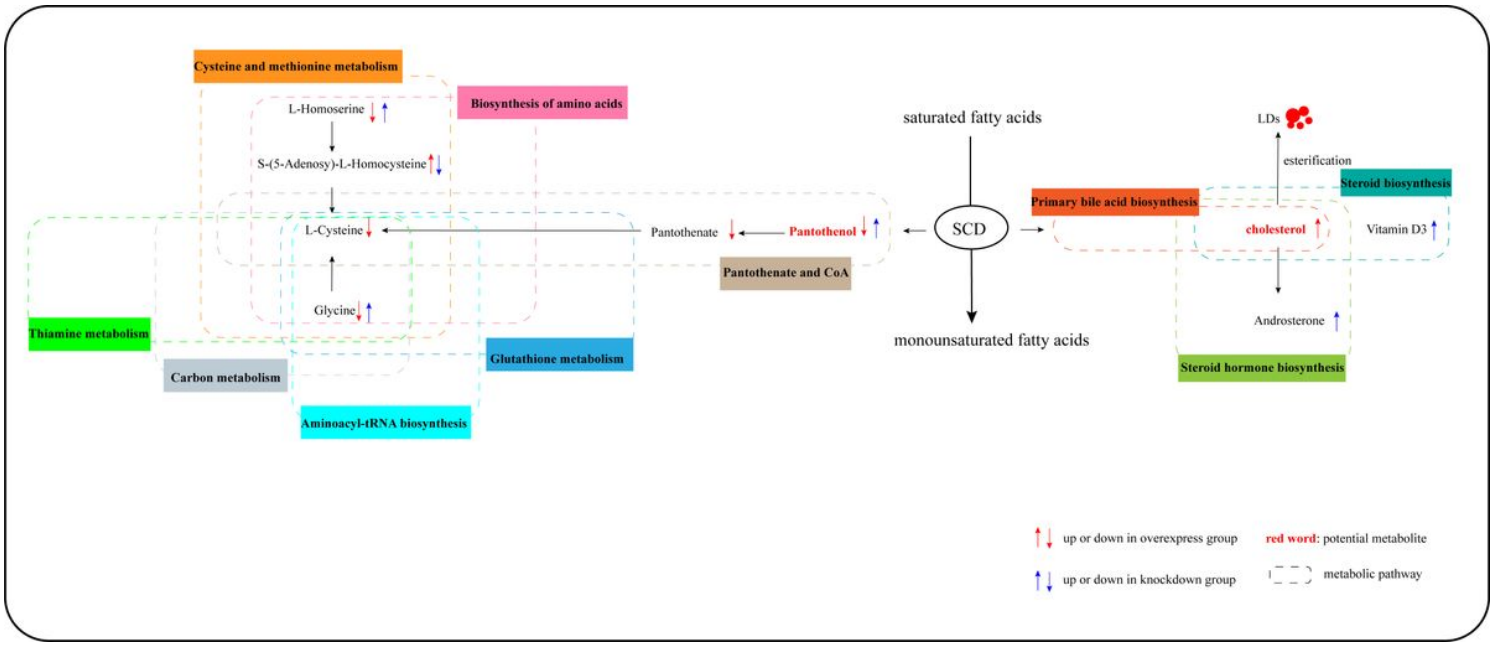

Figure 8

Potential metabolic pathway in goose GCs induced by overexpress and knockdown SCD. Notes: "↑" and "↓" in red indicate metabolic which in overexpress SCD group up- and down-regulated with the control group; "↑" and "↓" in blue indicate metabolic which in knockdown SCD group up- and down-regulated with the control group.

Supplementary Files

This is a list of supplementary files associated with this preprint. Click to download.

- TableS4.docx
- TableS3.docx
- TableS2.docx
- TableS1.docx
- FigureS1.pdf
- FigureS2.tif